Fresenius Z. Anal. Chem. 308, 195–200 (1981)

Fresenius Zeitschrift für Analytische Chemie

Session I. Physics and Technology of the Laser Microprobe Mass Analyzer LAMMA

LAMMA 500 Principle and Technical Description of the Instrument

H. Vogt, H. J. Heinen, S. Meier, and R. Wechsung

Leybold-Heraeus GmbH, Bonner Str. 504, D-5000 Köln 51, Federal Republic of Germany

LAMMA 500 — Prinzip und technische Beschreibung des Instruments

Key words: Massenspektrometrie, Lasermikrosonde; LAMMA 500, Gerätebeschreibung

Introduction

The Laser Microprobe Mass Analyzer LAMMA 500® [1] originally had been designed for the analysis of biomedical samples, especially thin sections, with high lateral resolution and extreme detection sensitivity [1]. The prinziple of LAMMA is based on the excitation of a microvolume of the sample to an ionized state by a focused laser beam. The analytical information is derived from mass spectrometry of these ions. It is obvious that all elements of the periodic table and their isotopes can be detected. Various applications have demonstrated that besides element detection the instrument can also be used for the detection of organic and inorganic compounds.

The application of LAMMA has meanwhile been extended from biological work to quite different fields such as general chemistry, mineralogy, criminology, geology, environmental research and others. It is a special feature of LAMMA that the analysis is performed under microscopic control. As electrical conductivity of the sample is no prerequisite for the ionization with a laser, non-conducting samples can be analyzed as well. In the following, a detailed description of the LAMMA 500 instrument will be given.

The LAMMA Instrument

The principle of the laser microprobe LAMMA 500 is shown in Fig. 1. A Nd:YAG-laser is used to generate very short and intense light pulses. The Q-switched oscillator has a "stable-resonator" design and provides approximately 25 mJ light energy in 15 ns at the infrared wavelength of 1060 nm. The intensity profile of the laser beam is approximately gaussian (TEM_{00}). An amplifier unit can increase the energy of the laser pulse by approximately a factor of four. Two thermostated frequency doubling crystals are used to generate the fourth harmonic of the fundamental wavelength. This gives a light pulse of about 2 mJ energy, delivered in a pulse time of 15 ns at the UV-wavelength of 265 nm. A He-Ne-laser continuously emitting in the red, is aligned collinear to the invisible UV-light of the Nd:YAG-laser. The He-Ne-laser beam eases the alignment of the UV-laser beam with respect to the axis of the microscope and serves for aiming at a selected area on the specimen. An intermediate optical system is used to expand the laser beam to the useful aperture of the objectives and to place the laser focus exactly into the intermediate image plane of the microscope objective.

An optical microscope with high resolving power (N.A. = 1.0) and a magnification of up to 1200 is used for sample observation. Incident and transmitted light illumination are standard, observation with phase contrast is also possible (option). UV-transmitting objectives are used for both sample observation and focusing of the laser beam. With an 100 × objective the nominal diameter of the laser focus on the sample is approximately 0.5 μm. Because of a number of physical effects, the area of damaged and/or evaporated sample material is, in most practical applications, somewhat larger. For organic samples, analyzed at an irradiance of about 3–5 times threshold, the perforations have a diameter of typically 1 μm. The diameter increases further with increasing irradiance. Maximum power density in the focus is 10^{11} W/cm^2. It can be reduced by a set of attenuating filters.

Because of the mass spectrometric analysis the sample has to be placed into the vacuum. It is usually transferred onto a coated electromicroscopical grid that fits into the $x-y$ movable sample stage. A

1 LAMMA® is a registered trade mark of Leybold-Heraeus GmbH

0016-1152/81/0308/0195/$01.20

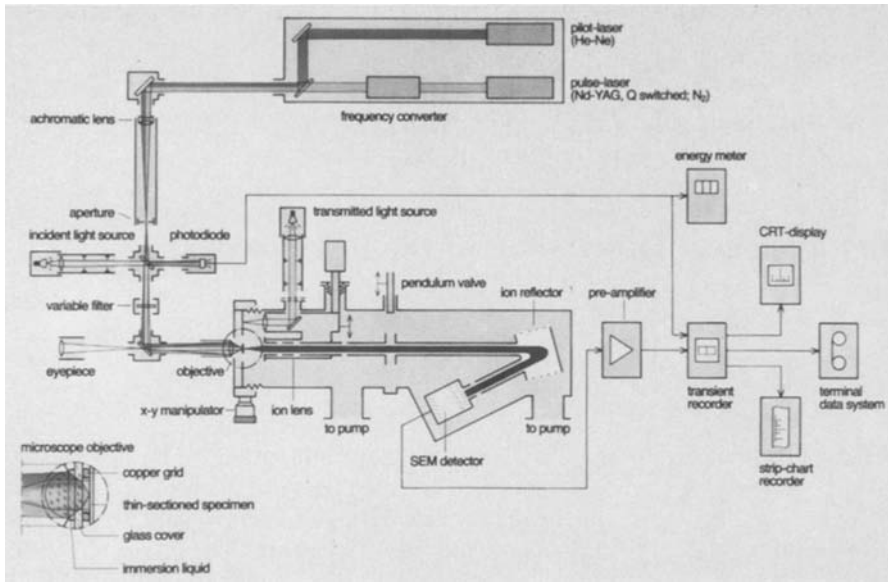

Fig. 1. Schematic diagram of LAMMA 500

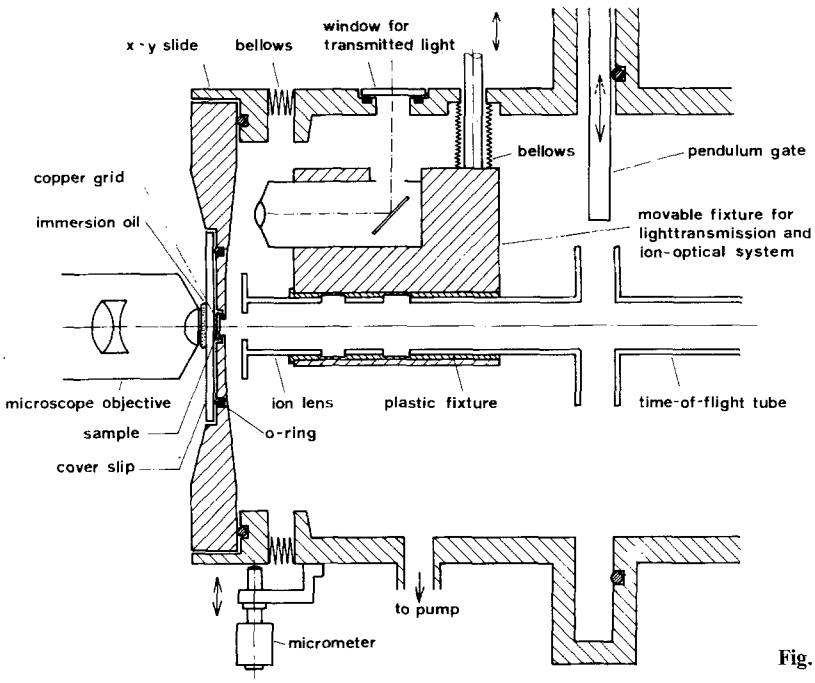

Fig. 2. Drawing of the sample chamber

standard quartz cover slide serves as vacuum seal and optical window (see insert to Fig. 1 and Fig. 2). The EM-grid separates the sample from the cover slide by approximately 20 µm, thereby preventing the window from getting damaged and contributing background signals to the spectrum. Positioning of the sample location, selected for analysis, is done by two micrometer screws with a lateral positioning accuracy of 0.5 µm. For focusing of the laser beam the objective is moved until the focus of the He-Ne-laser on the sample surface has a minimum diameter.

For analysis, the transmitted light condenser which, for observation, is located directly behind the sample, is replaced by an ion optic system. This is done electropneumatically by pushbutton operation and needs only fractions of a second. The ions which are formed by laser irradiation of the selected sample area are accelerated into the mass spectrometer. An "einzel-lens" is used to increase the acceptance of the time-of-flight spectrometer. In Fig. 3 the effect of the ion acceleration stage and the "einzel-lens" on the ion paths is shown.

The time-of-flight mass spectrometer to be described in detail further down, can be used for positive or negative ion detection, depending on the polarity of the potentials at the electrodes. An open secondary

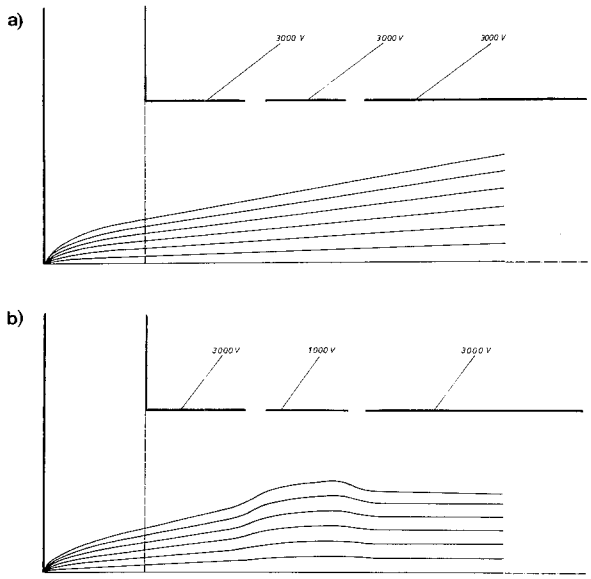

Fig. 3. Traces of the ions in the sample chamber **a** without, and **b** with the action of the "einzel-lens"

electron multiplier with 17 CuBe dynodes is used for ion detection. The potential of the ion collector electrode can be set separately to ensure an efficient ion-to-electron conversion and to reduce mass discrimination. The 17 stage multiplier has a gain of 10^6 or better. In cases of large ion currents, for which saturation of the last SEM-stages would distort the spectra, the signal can be tapped at the 6th or 12th SEM stage. The analogue signal of the detector is digitized with 8 bit resolution and stored in a transient recorder of 2 k channels. Sample intervals are usually 10, 20 or 50 ns. The selected delay time and sampling rate determine the recorded mass range and to some degree the achieved mass resolution. The recorded spectrum is displayed on a CRT-screen. It can be plotted by a strip chart recorder or transferred to a data system.

A turbomolecular pump is used for evacuation of the system. For sample exchange the spectrometer and detector section is closed off by a pendulum valve and kept at the working pressure of $10^{-7}-10^{-6}$ mbar by an ion getter pump. The sample chamber can then be vented with dry nitrogen. After sample exchange, the sample chamber is evacuated by the turbomolecular pump to some 10^{-6} mbar within a few minutes. All vacuum pumps, the valves and the high voltage power supply are controlled by an electronic interlock system to prevent accidental operational mistakes.

Sample Insertion

The LAMMA sample chamber has been designed for the analysis of thin sections, mounted on 3 mm grids as used in electron microscopy. However, other types of samples can be mounted and analyzed as well:

I. Particles with diameters between 0.2 μm and about 20 μm can be impacted onto a thin (ca. 200 Å) polymer film (Formvar or Collodium) on a supporting grid.

II. Another possibility is to attach particulate material directly to a blanc grid by bringing it into contact with the powder. Some particles always adhere within a grid mesh and can be analyzed directly without background signals from the supporting film.

III. Particles of a size between 0.1 – 1 mm can be inserted into a "sandwich grid". They have to be analyzed with laser light at grazing incidence at a visible edge.

IV. Samples of a few millimeters size can be fixed to the back side of the sample holder with adhesive tape. Due to the distance between the sample and the objective, the observation is in this case limited to magnifications of 125 – 350 times, giving a lateral resolution of approximately 2 – 3 μm. These samples also can be analyzed in grazing incidence only.

The Time-of-Flight Mass Spectrometer (tof-ms)

By the interaction of the light pulse of a Q-switched laser with the thin specimen, ion formation is induced within a time interval of the order of the laser pulse duration (10 – 20 ns). An electrostatic tof-ms provides two particular advantages over other types of mass analyzers:

I. From a single laser pulse, a whole mass spectrum of one polarity can be recorded. There are no ion losses due to dead times of scanning.

II. Consisting essentially of cylindrical tube electrodes, the tof-ms has a high transmittance for the ions. This leads to the high detection sensitivity of the instrument.

The mass dispersion of a tof-ms is due to the fact that ions of a given kinetic energy have different velocities depending on their mass. For a first approximation the time necessary to accelerate the ions in the sample chamber by an electric potential U_{tof} as well as the influence of the initial kinetic energies E_0, due to the laser ionization process, are neglected in the following. After the acceleration, the ions have kinetic energies

$$E_{\text{K}} = \frac{1}{2} m v^2 = q \cdot U_{\text{tof}} \tag{1}$$

where q is the charge of the particle. This leads to

$$v = \sqrt{2 q U_{\text{tof}}/m}\,. \tag{2}$$

Thus, the ions need different times to reach the detector as illustrated in Fig. 4. It follows directly that

$$t_{\text{drift}} = C \cdot \sqrt{m}\,. \tag{3}$$

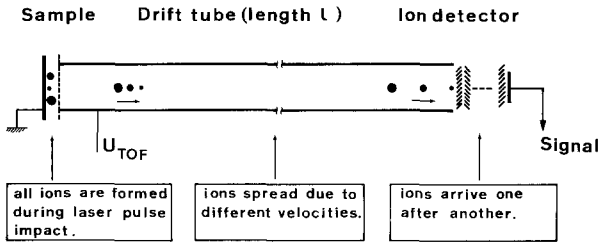

Fig. 4. Principle of a time-of-flight mass spectrometer

The constant C can be calculated from the geometry and the electric potentials of the tof-ms. In practice, however, it is easier to derive the value of C from one or several identified peaks of a mass spectrum obtained for example from a standard sample (Fig. 9).

The mass resolution A at mass m is given by the separation Δt of two adjacent masses ($\Delta m = 1$) and the peak half width δt:

$$A = \frac{\Delta t}{\delta t} \cdot \frac{m}{\Delta m}. \tag{4}$$

For a good approximation Δt is given by

$$\Delta t \sim L/\sqrt{U_{\text{tof}} \cdot m} \tag{5}$$

where L is the length of a straight drift tube. It is important to realize that Δt decreases with $1/\sqrt{U_{\text{tof}}}$ and $1/\sqrt{m}$.

The peak width δt is influenced by the distribution of initial energies E_0 of the ions, by differences in drift times for different ion paths, by the length of the ion acceleration and drift path and by the response time c_A of the ion detection system. Thus

$$\delta t = f(\Delta E_0,\ c_A,\ m,\ U_{\text{tof}}). \tag{6}$$

The initial energy E_0 results from the laser ionization process and depends on the excitation state of the sample which in turn is influenced by the laser intensity applied and the absorption characteristic of the irradiated sample area. For non metallic thin samples, E_0 is usually below 20 eV. For bulk samples, especially metals, E_0 can increase up to several hundred eV (2) which cannot be considered small with respect to the ion accelerating potential U_{tof}.

The instrumental response time c_A is essentially influenced by the transit-time spread of the multiplier, and the frequency bandwidth of the preamplifiers. The instrumental response time of the multiplier and preamplifier is typically around 10^{-8} s. The analogue to digital converter with its maximum sampling rate of 1 per 10 ns is therefore the limiting element. If e. g. one requires a minimum of 5 sample intervals per peak half width δt, any t below 50 ns would lead to a loss in fidelity of the peak amplitude or peak area. In Fig. 5 the influence of the response time c_A on the mass resolution is shown.

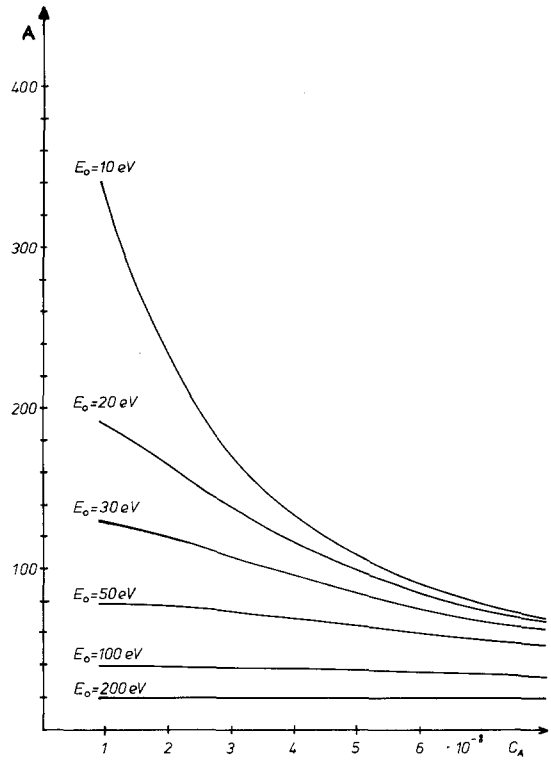

Fig. 5. Dependence of the mass resolution of a linear tof-ms of length L = 1 m on the response time c_A for ions of mass 100 amu with various initial energies (theoretical). The potential of the drift tube is 4 kV

As can be seen from the above explanations, there is an optimum for the mass resolution as a function of U_{tof} for any given response time c_A. This dependence is shown in Fig. 6.

The contribution of ΔE_0 to the peak width δt decreases faster with increasing U_{tof} than the time separation Δt of adjacent peaks of mass difference Δm, thereby leading to an increasing resolution A with incresing U_{tof}. Eventually the contributions to δt from c_A dominate and further increase of U_{tof} would lead to a decrease in A because of the still further decreasing Δt.

The mass resolution of a tof-ms can be considerably improved by employing an ion reflector system in the drift path (Fig. 1) for the following reasons:

I. For the same instrument size, the length of the drift path and thus the mass dispersion are nearly doubled compared to a linear tof-ms.

II. Differences in drift times in the field free parts of the tof-ms, due to different initial energies of the ions, can be compensated by different path lengths in the ion reflector (energy-time focusing).

In effect the dependence of the sample excitation conditions on the mass resolution is strongly reduced (Fig. 7).

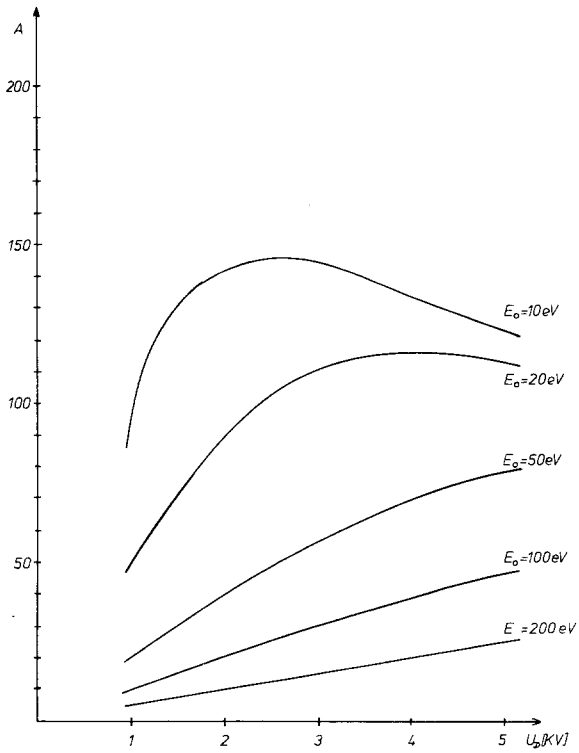

Fig. 6. Dependence of the mass resolution of a linear tof-ms of length $L = 1$ m on the acceleration potential for ions of mass 100 amu with various initial energies (theoretical). $c_A = 4 \times 10^{-8}$ s

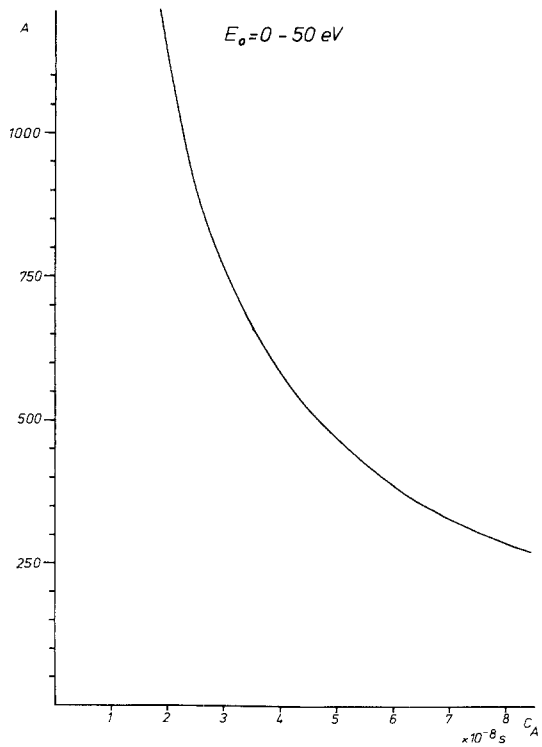

Fig. 7. Dependence of the mass resolution of a tof-ms with an ion reflector on the response time c_A for ions of mass 100 amu (theoretical). $U_{tof} = 1$ kV; $L_{eq} = 2$ m

Due to the larger equivalent drift length L_{equ}, also the maximum mass resolution is increased. In principle, there is no upper limit for the detectable mass range as the ion paths in the tof-ms are independent of the mass of the ions. Practical limits are given by the decreasing possibility to resolve peaks of adjacent mass numbers e.g. in isotopic patterns with increasing mass [eq. (5)] and by the limited capacity of the buffer store. With LAMMA 500, masses up to 1000 amu have been detected.

Due to the high transmittance of the tof-ms in LAMMA, between one and ten percent of the total number of ions formed in the laser focus are usually detected by the secondary electron multiplier. Thus, elemental detection limits are in the low ppm (weight) concentration range, at least in an organic matrix, which corresponds to a few thousand atoms in a sample volume of approximately 1 μm^3. As single ions can in principle be recorded with LAMMA, the detection limits are in practice mainly determined by mass spectrometric background, i. e. interference of small organic fragment ions of the same nominal mass as the isotope to be detected.

Analysis of a Doped Epoxy Resin Foil

The performance of the LAMMA instrument is demonstrated by the spectrum obtained from a 0.3 μm thick section of "Spurr's low viscosity medium", an epoxy resin, frequently used for embedding biological material for X-ray microprobe analysis. The analyzed resin had been doped with the elements Li, Na, K, Sr, and Pb at a concentration of 10^{-2} mole/l. Such specimens have been developed to serve as standard samples for a variety of LAMMA analyses. Fig. 8 shows a micrograph of the foil with a series of laser perforations. Corresponding mass spectra are shown in Fig. 9. Besides atomic ions of the doping elements, a characteristic fragment ion spectrum from the epoxy polymer can be seen. In favourable cases, the mass resolution can be increased to resolve, at least partially, mass doubletts in the low mass range. As can be seen in Fig. 10, two different ions contribute to the signal at mass 41. A careful evaluation revealed that these ions should be $41K^+$ and $C_3H_5^+$. This assignement is also supported by the fact that the intensity of the peaks 39 and 41 a reflect the natural abundance of the K isotopes [3].

The contributions to this volume prove that within two years after its introduction to the analytical market, LAMMA has been accepted and saluted as a new method and a unique instrument. Although a considerable number of applications in quite different

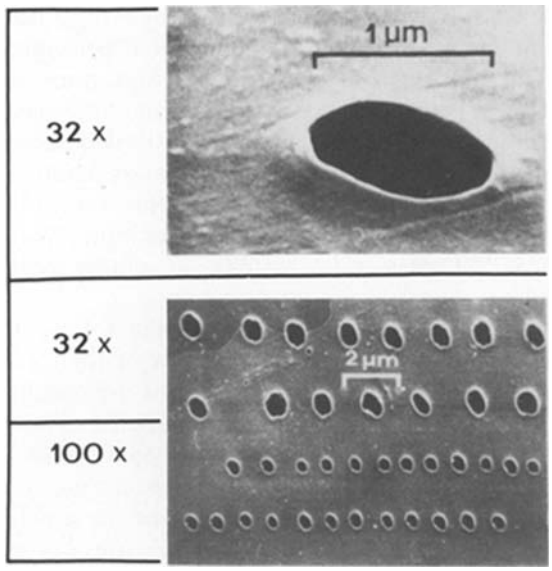

Fig. 8. Electron micrograph of an epoxy polymer thin section with a series of laser perforations. Top perforation and top two lines of lower part were obtained with an 32 × objective, the bottom two lines of perforations with an 100 × objective

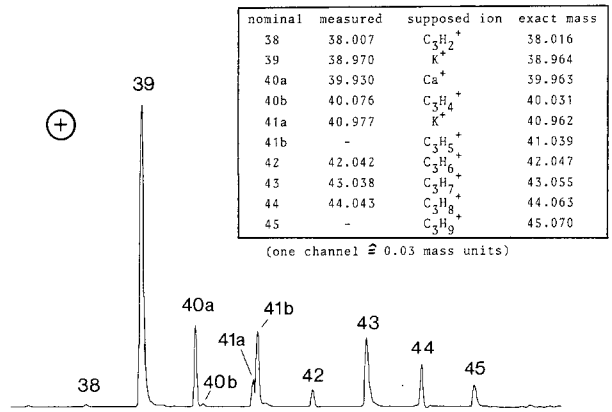

nominal	measured	supposed ion	exact mass
38	38.007	$C_3H_2^+$	38.016
39	38.970	K^+	38.964
40a	39.930	Ca^+	39.963
40b	40.076	$C_3H_4^+$	40.031
41a	40.977	K^+	40.962
41b	-	$C_3H_5^+$	41.039
42	42.042	$C_3H_6^+$	42.047
43	43.038	$C_3H_7^+$	43.055
44	44.043	$C_3H_8^+$	44.063
45	-	$C_3H_9^+$	45.070

(one channel ≙ 0.03 mass units)

Fig. 10. Part of the spectrum with ultimate mass resolution

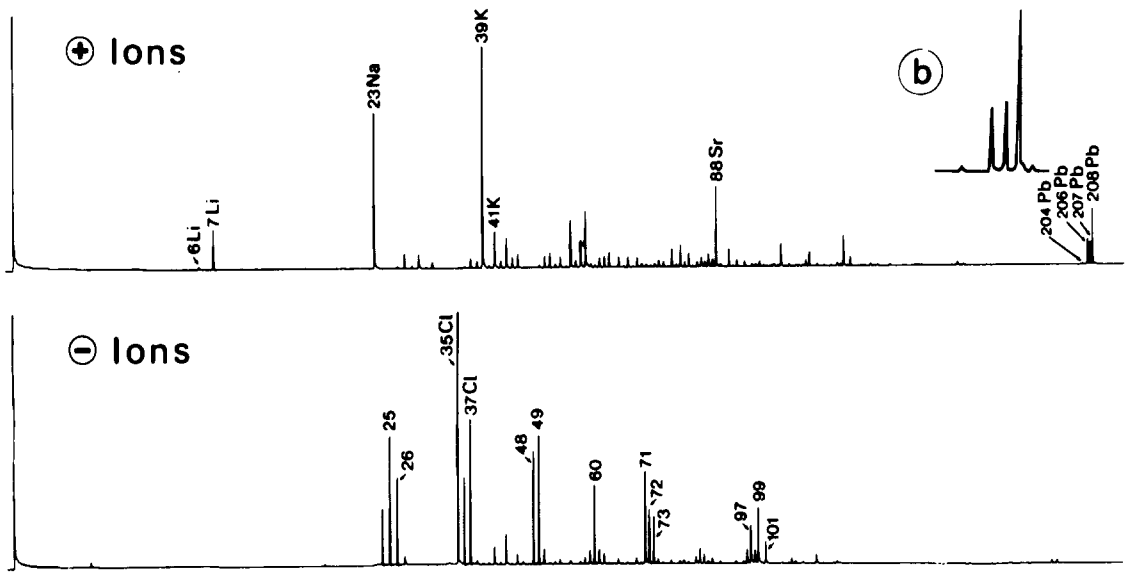

Fig. 9. LAMMA spectra of a thin section of "Spurr's low viscosity medium" doped with Li, Na, K, Sr, and Pb as crown ether complexes at a concentration of 10^{-2} mole/l. **b** = lead isotopes, recorded with high sampling rate

areas of research have already been carried out, a further extension to new areas is still to be expected.

References

1. Hillenkamp, F., Unsöld, E., Kaufmann, R., Nitsche, R.: Appl. Phys. **8**, 341–348 (1975)
2. Ready, J. F., Effects of high-power laser radiation. London 1971. Acad. Press.
3. Heinen, H. J., Meier, S., Vogt, H., Wechsung, R.: Proc. Int. Vac. Congr., Cannes (France), 22.–26. Sept. 1980

Received May 7, 1981